Supporting information

Efficient Solar-driven Hydrogen Generation Using Colloidal Heterostructured Quantum Dots

Kanghong Wang [a,b], Xin Tong [b,c], Yufeng Zhou [b], Hui Zhang [b], Fabiola Navarro Pardo [b,c], Gurpreet S. Selopal [b,c], Guiju Liu [d], Jie Tang [d], Yiqian Wang [d], Shuhui Sun [b], Dongling Ma [b], Zhiming M. Wang [c], François Vidal [b], Haiguang Zhao [d,*], Xuhui Sun [a,*], and Federico Rosei [b,c,*]

[a] Institute of Functional Nano & Soft Materials (FUNSOM), Soochow University, Suzhou, Jiangsu 215123, People's Republic of China.

[b] Institut National de la Recherche Scientifique, Centre Énergie, Matériaux et Télécommunications, 1650 Boul. Lionel Boulet, J3X 1S2 Varennes, Québec, Canada.

[c] Institute of Fundamental and Frontier Sciences, University of Electronic Science and Technology of China, Chengdu 610054, People's Republic of China.

[d] The State Key Laboratory and College of Physics, Qingdao University, No. 308 Ningxia Road, Qingdao 266071, PR China

*Corresponding authors: hgzhao@qdu.edu.cn , xhsun@suda.edu.cn , rosei@emt.inrs.ca

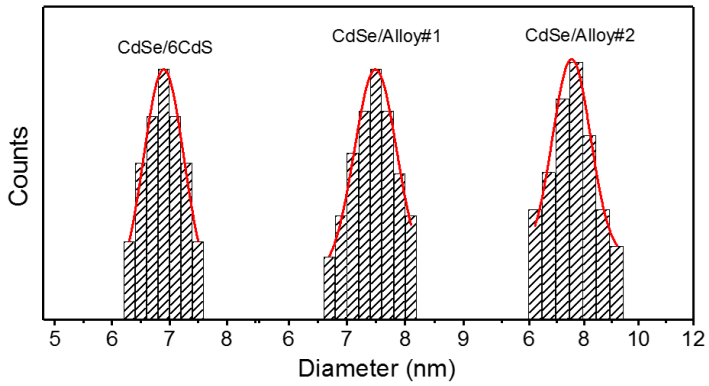

Figure S1. Size distribution of CdSe/6CdS, CdSe/Alloy#1 and CdSe/Alloy#2 QDs.

Table S1. Size distribution for CdSe/6CdS, CdSe/Alloy#1 and CdSe/Alloy#2 QDs

Core/Shell QDs structure	D* (nm)	H* (nm)	Overall size (nm)
CdSe/6CdS	3.3	1.96	7.2±0.5
CdSe/Alloy#1	3.3	2.07	7.7±0.8
CdSe/ Alloy#2	3.3	2.50	7.9±0.9

[a]D is the CdSe core diameter and [b]H is the shell thickness

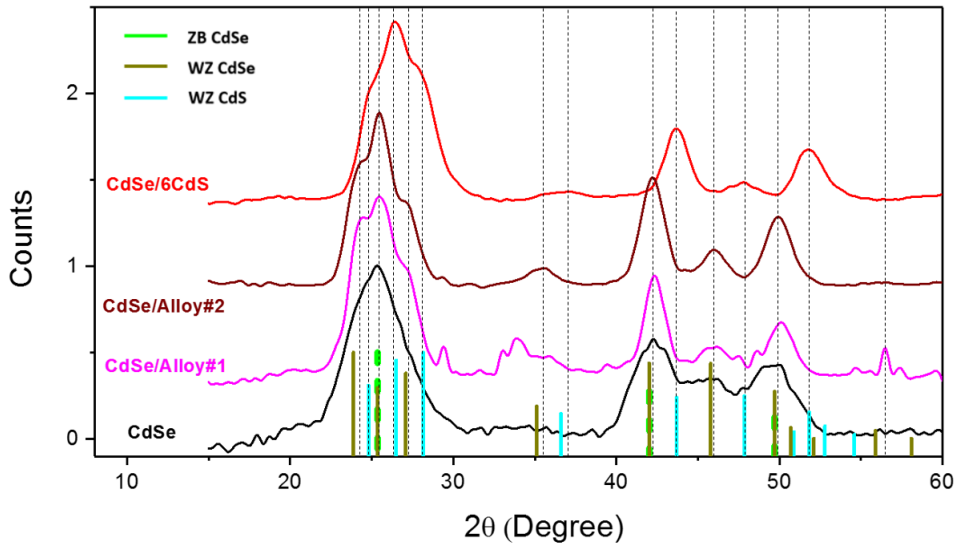

Figure S2. XRD pattern of CdSe, CdSe/6CdS, CdSe/Alloy#1 and CdSe/Alloy#2 QDs.

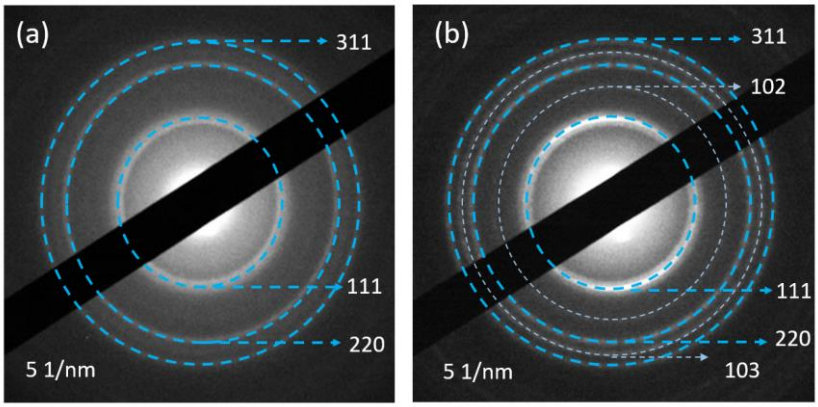

Figure S3. Selected area electron diffraction pattern: (a) CdSe/Alloy#1 QDs (b) CdSe/Alloy#2 QDs.

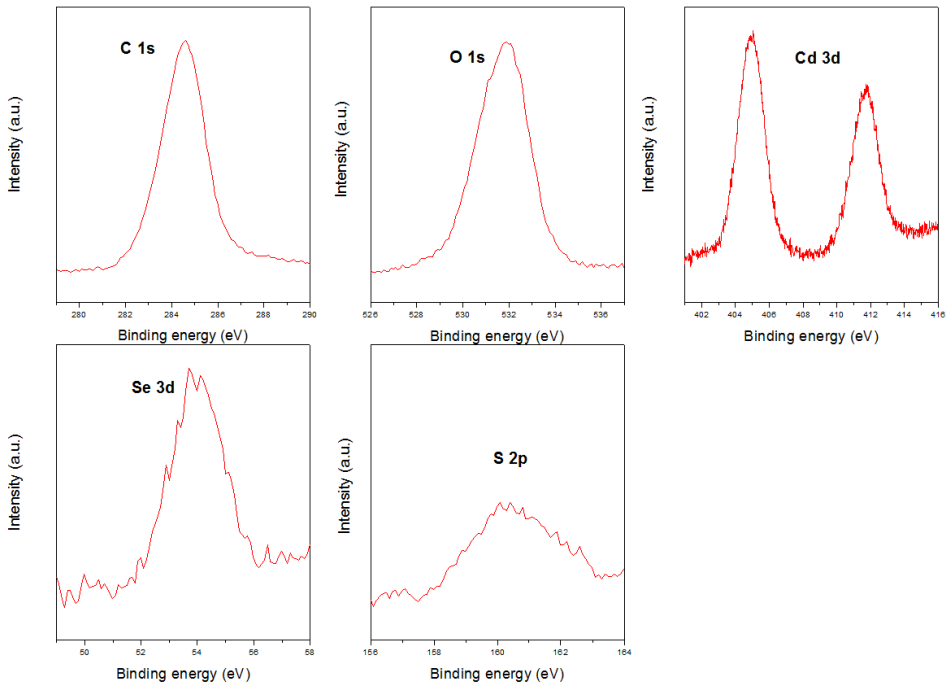

Figure S4. XPS spectra of CdSe/Alloy#2 QDs.

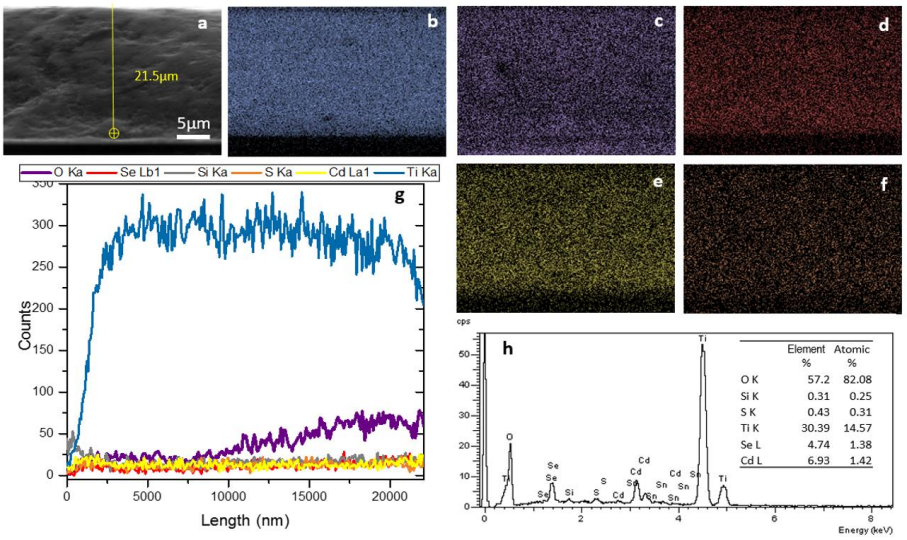

Figure S5. (a) Cross-sectional SEM image of CdSe/CdS QD-sensitized photoanode. EDS mapping analysis of all the elements including (b) Ti, (c) O, (d) Se (e) Cd and (f) S. (g) EDS line mapping of the highlighted path in the SEM image and (h) EDS spectrum.

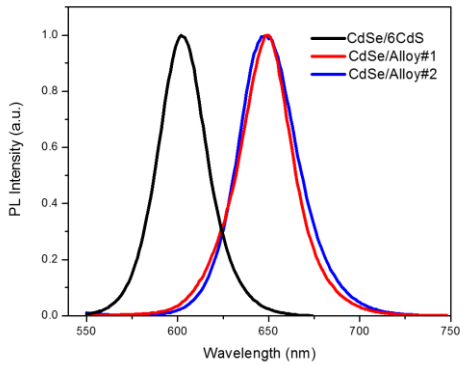

Figure S6. PL spectra of CdSe/6CdS, CdSe/Alloy#1 and CdSe/Alloy#2 QDs in the toluene.

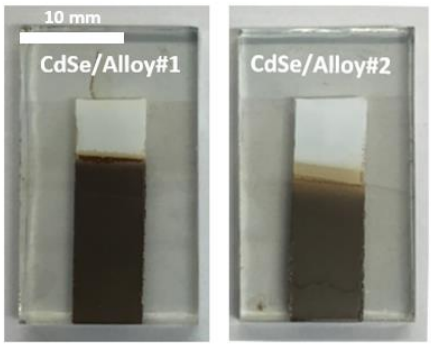

Figure S7. Samples CdSe/Alloy#1 and CdSe/Alloy#2 QDs after deposition in TiO_2 through EPD process (scale bar shown in the image).

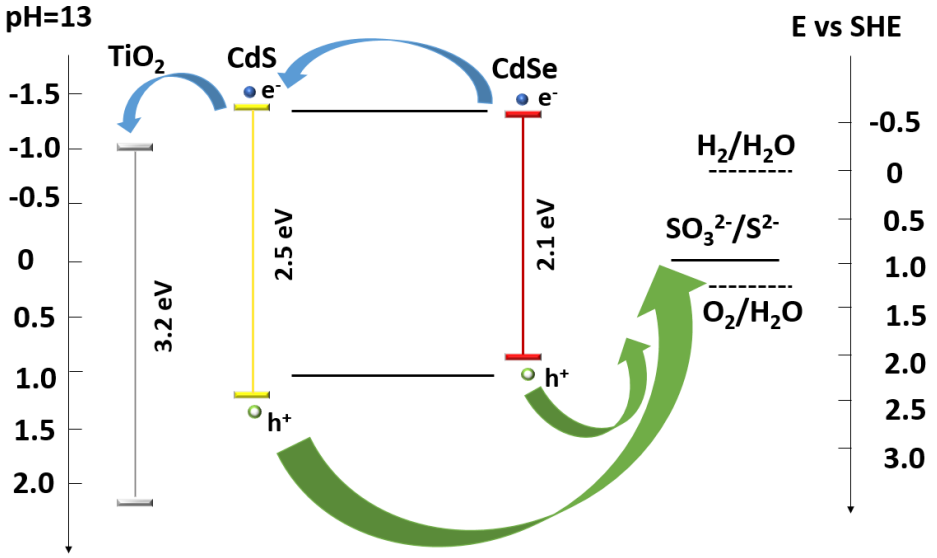

Figure S8. Charge transition diagram of CdSe/Alloy#1 based photoanode.

Table S2. The radius of core, thickness of shell and e-h spatial overlapping values for CdSe/6CdS, CdSe/Alloy#1 and CdSe/Alloy#2 QDs.

Core/Shell QDs structure	R* (nm)	H* (nm)	e-h overlapping area (10^{-10}cm^2 %)
CdSe/6CdS	1.65	1.96	64
CdSe/Alloy#1	1.65	2.07	67
CdSe/ Alloy#2	1.65	2.50	70

Calculation of e-h spatial overlapping area value:

For the e-h spatial overlapping area, first we plotted the spatial probability distribution value of electron and hole as the function of QDs radius in the origin file.

Then we calculated the overlap areas value ($S_{overlap}$) of electron and hole wave function. In addition, we calculated the overall areas value ($S_{overall}$) of electron and hole wave function.

Finally, we calculated the value of the overlap areas account for the overall areas under the curve which is the e-h spatial overlapping area value ($\frac{S\,overlap}{S\,overall}$).

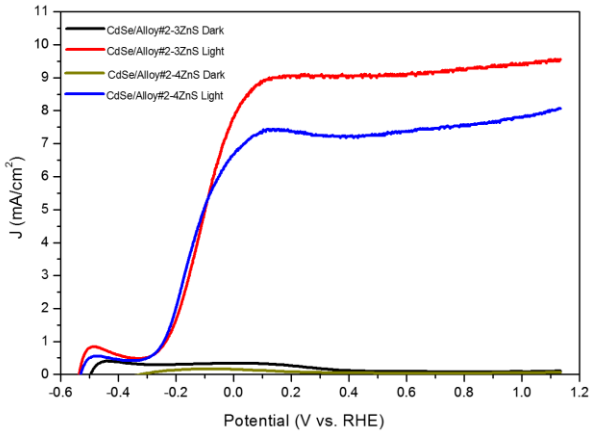

Figure S9. Photocurrent density versus bias potential (versus RHE) for TiO_2/CdSe/Alloy#2 with 3 and 4 cycles of ZnS photoanodes in the dark and under continuous illumination (AM 1.5 G, 100 mW/cm^2).

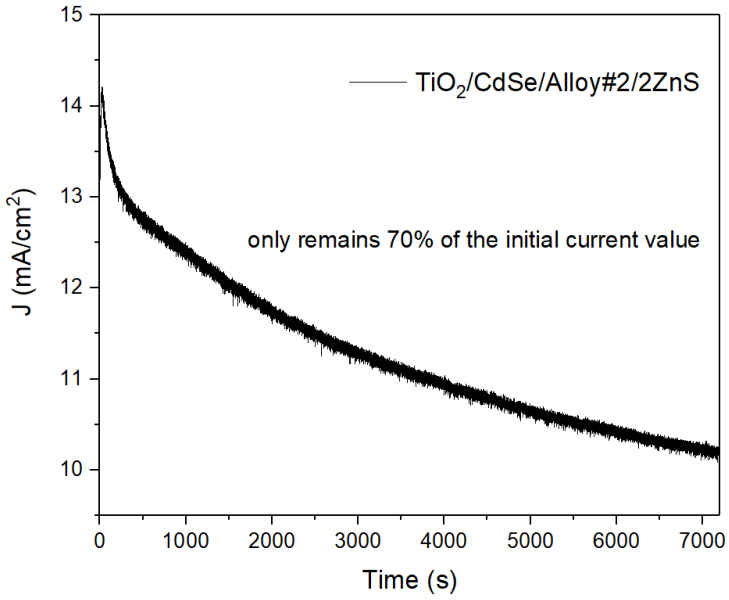

Figure S10. Stability spectra of the sample CdSe/Alloy#2 with 2 cycles of ZnS coating.

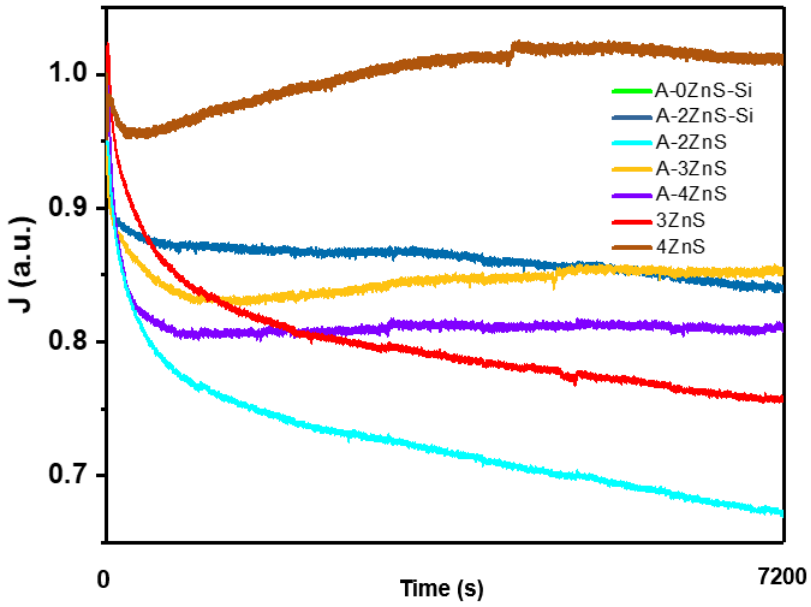

Figure S11. Normalized stability spectra of the sample CdSe/Alloy#2 with different treatment (Annealing, different cycles of ZnS coating and SiO_2 coating).

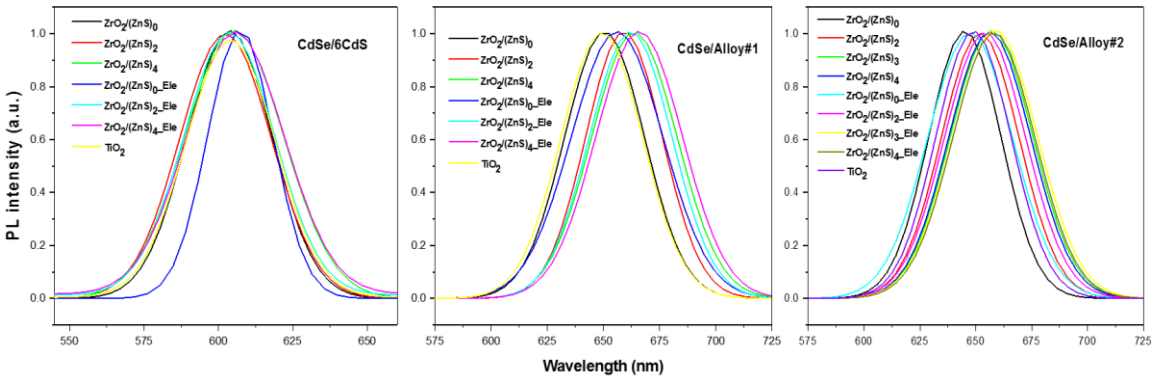

Figure S12. PL spectra of CdSe/6CdS, CdSe/Alloy#1 and CdSe/Alloy#2 QDs as function of different cycles (thickness) of ZnS.

In table S3 and Fig S12, with the increasing of ZnS thickness, the electron lifetime with ZrO_2 and lifetime with electrolyte are both prolonged due to the thicker ZnS layers. As a result, the hole transfer rate calculated by the previous two values are decreased as the increasing thickness of ZnS layers.

In Fig S12, for CdSe/6CdS QDs, the peak position and intensity in PL spectra are almost the same with the different cycles of ZnS, except 0ZnS with electrolyte which may contribute to none protection of ZnS, leading to quenching to QDs of strong alkaline electrolyte. While for two types of alloyed QDs, the PL peak position will shift obviously as function of different ZnS cycles compared to CdSe/6CdS QDs. This is because the favorable band alignment will increase the mobility of carriers.

Basically, with the increasing of ZnS cycles, or addition of electrolyte, the PL peak will shift to longer wavelength due to more leakage of electrons into shell regions which is consistent with the results in table S3.

Table S3. Lifetime in ZrO_2 with and without electrolyte and corresponding hole transfer rate for CdSe/6CdS, CdSe/Alloy#1 and CdSe/Alloy#2 QDs with different cycles of ZnS coating

Sample	Lifetime with ZrO_2 (ns)	Lifetime with electrolyte (ns)	Hole transfer rate H (10^7/s)
CdSe/6CdS-0ZnS	25	8	8.5
CdSe/6CdS-2ZnS	24	10	5.8
CdSe/6CdS-4ZnS	30	10	6.7
CdSe/Alloy#1-0ZnS	22	7	9.7
CdSe/Alloy#1-2ZnS	21	8	7.7
CdSe/Alloy#1-4ZnS	24	10	5.8
CdSe/Alloy#2-0ZnS	23	8	8.2
CdSe/Alloy#2-2ZnS	15	8	5.8
CdSe/Alloy#2-3ZnS	21	11	4.3
CdSe/Alloy#2-4ZnS	20	10	5.0

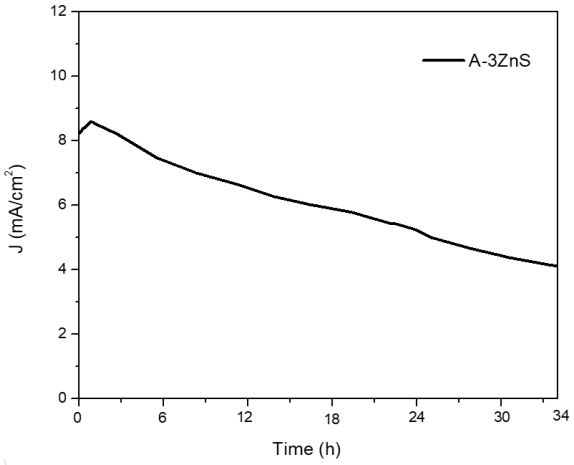

Figure S13. Stability spectra of the sample CdSe/Alloy#2 with the annealing-3 cycles of ZnS treatment.

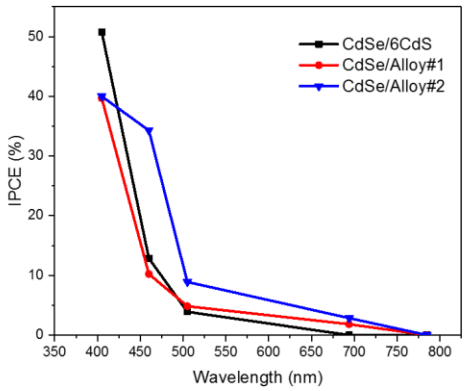

Figure S14. IPCE spectra for CdSe/6CdS, CdSe/Alloy#1 and CdSe/Alloy#2 QDs.

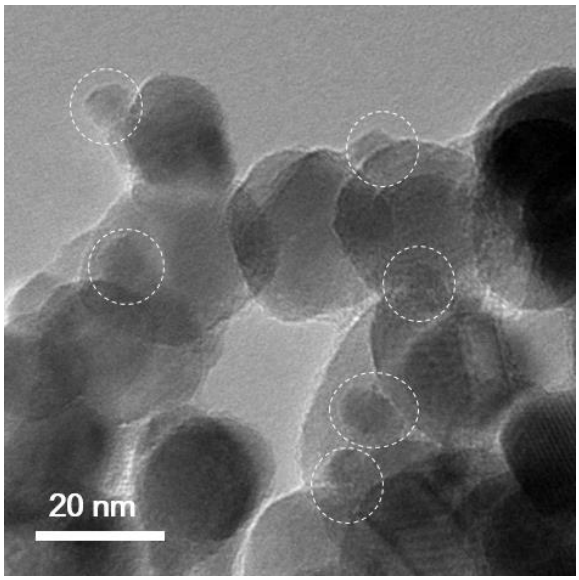

Figure S15. TEM image of CdSe/Alloy#2 QDs with ZrO_2 thin film (the white circles shown the QDs).